AGRO100 inhibits activation of nuclear factor-κB (NF-κB) by forming a complex with NF-κB essential modulator (NEMO) and nucleolin

Allicia C. Girvan,[1] Yun Teng,[2] Lavona K. Casson,[2] Shelia D. Thomas,[2] Simone Jüliger,[2] Mark W. Ball,[2] Jon B. Klein,[2] William M. Pierce, Jr.,[3] Shirish S. Barve,[2,3] and Paula J. Bates[1,2]

Departments of [1]Biochemistry and Molecular Biology, [2]Medicine, and [3]Pharmacology and Toxicology, James Graham Brown Cancer Center, University of Louisville, Louisville, Kentucky

Abstract

AGRO100, also known as AS1411, is an experimental anticancer drug that recently entered human clinical trials. It is a member of a novel class of antiproliferative agents known as G-rich oligonucleotides (GRO), which are non-antisense, guanosine-rich phosphodiester oligodeoxynucleotides that form stable G-quadruplex structures. The biological activity of GROs results from their binding to specific cellular proteins as aptamers. One important target protein of GROs has been previously identified as nucleolin, a multifunctional protein expressed at high levels by cancer cells. Here, we report that AGRO100 also associates with nuclear factor-κB (NF-κB) essential modulator (NEMO), which is a regulatory subunit of the inhibitor of κB (IκB) kinase (IKK) complex, and also called IKKγ. In the classic NF-κB pathway, the IKK complex is required for phosphorylation of IκBα and subsequent activation of the transcription factor NF-κB. We found that treatment of cancer cells with AGRO100 inhibits IKK activity and reduces phosphorylation of IκBα in response to tumor necrosis factor-α stimulation. Using a reporter gene assay, we showed that AGRO100 blocks both tumor necrosis factor-α-induced and constitutive NF-κB activity in human cancer cell lines derived from cervical, prostate, breast, and lung carcinomas. In addition, we showed that, in AGRO100-treated cancer cells, NEMO is coprecipitated by nucleolin, indicating that both proteins are present in the same complex. Our studies suggest that abrogation of NF-κB activity may contribute to the anticancer effects of AGRO100 and that nucleolin may play a previously unknown role in regulating the NF-κB pathway. [Mol Cancer Ther 2006;5(7):1790–9]

Introduction

Many common types of cancer, especially in their advanced stages, do not respond well to traditional chemotherapy agents or may acquire resistance to therapy. Novel agents that work by mechanisms that are different from existing therapies, particularly those that are able to target multiple pathways important for cancer cell survival, may therefore be useful in the treatment of advanced cancer. We have reported previously that certain guanosine-rich phosphodiester oligodeoxynucleotides, termed G-rich oligonucleotides (GRO), have antiproliferative activity against a variety of cancer cell lines (1–4). Furthermore, an active GRO (named GRO29A) can cause cell cycle arrest and induction of cell death in human cancer cell lines but not in non-malignant human cells (4). Following preclinical *in vivo* studies, which showed that it had no detectable toxicity in normal tissues (5), a truncated version of GRO29A, known as AGRO100 (recently renamed AS1411), has been tested in a phase I clinical trial of patients with advanced cancer. The results of this trial were recently presented (6) and indicated that AGRO100 was well tolerated (no serious adverse effects were observed) and had promising clinical activity.

In previous studies, we have examined a series of G-rich sequences to determine a structure-activity relationship and to gain insight into their novel mechanism (1–3). We found that active GROs can have diverse G-rich sequences, but all could adopt folded conformations that are stabilized by G-quartets. However, formation of a stable G-quadruplex was not sufficient for activity. In addition, there was a very good correlation between the biological activity of GROs and their abilities to form a specific complex containing a protein that was identified as nucleolin (1–3). There is strong evidence from UV cross-linking and Southwestern blotting (1) that GROs bind directly to nucleolin rather than interact through an intermediary protein; therefore, we have proposed that nucleolin is the primary target of GROs, such as AGRO100.

Despite their probable target having been identified, the detailed mechanism of action for GROs is not yet fully understood. In part, this is because little is known about the role of nucleolin in cancer biology. Nucleolin protein is expressed at high levels in rapidly proliferating cells, such

Received 9/8/05; revised 5/4/06; accepted 5/16/06.

Grant support: Department of Defense Prostate Cancer Research Program grants PC001482 and PC030134 (P.J. Bates), Susan G. Komen Breast Cancer Foundation grant DISS0202095 (P.J. Bates), IMD3 Fellowship (A.C. Girvan and M.W. Ball), and Commonwealth of Kentucky Research Challenge Trust and the Brown Cancer Center.

The costs of publication of this article were defrayed in part by the payment of page charges. This article must therefore be hereby marked advertisement in accordance with 18 U.S.C. Section 1734 solely to indicate this fact.

Requests for reprints: Paula J. Bates, University of Louisville, 580 South Preston Street, Delia Baxter Building 321, Louisville, KY 40202-1756. Phone: 502-852-2432; Fax: 502-852-2356.
E-mail: paula.bates@louisville.edu

Copyright © 2006 American Association for Cancer Research.

doi:10.1158/1535-7163.MCT-05-0361

Downloaded from mct.aacrjournals.org on April 10, 2020. © 2006 American Association for Cancer Research.

as cancer cells (7), and nucleolin is a major component of a set of cancer prognostic markers (silver-staining nucleolar organizer regions) whose levels are elevated in cancer cells compared with normal or premalignant cells (8, 9). Although it is best known as a nucleolar protein with a role in ribosome biogenesis, nucleolin is in fact a remarkably multifunctional protein that can also be present in the nucleoplasm, cytoplasm, and on the cell surface (10–15). In addition to its multiple functions in ribosome biogenesis (10–12), nucleolin is thought to play a role in numerous cellular processes, including apoptosis (16), signal transduction (14, 17–19), DNA replication (20, 21), mRNA stability (22–24), protein trafficking (13, 25), stress response (26, 27), and telomerase function (28). It has been reported by several research groups that nucleolin binds to G-quadruplex-forming DNA sequences, such as the human telomere (29, 30), immunoglobulin switch regions (31), and rDNA (32), but the significance of these interactions *in vivo* has not yet been determined.

Recently, we identified nuclear factor-κB (NF-κB) essential modulator [NEMO; also known as inhibitor of κB (IκB) kinase (IKK) γ and IKKAP1] as a potential GRO-associated protein following mass spectrometry analysis of proteins that were precipitated when an active biotin-linked GRO was incubated with cancer cell extracts.[4] It was selected for further investigation because of its important role in NF-κB signaling, a pathway that is often deregulated in cancer cells (33–35) and that has been reported previously to be inhibited by polyguanosine sequences (36, 37) via an uncharacterized mechanism. ''NF-κB'' refers to a family of proteins that function as dimeric transcription factors to affect the expression of genes involved in immune and inflammatory responses, cell growth, differentiation, and apoptosis (34, 38, 39). In nonstimulated cells, NF-κB is normally bound to an inhibitor called IκBα, which sequesters it in the cytoplasm in an inactive state. On ligation of an appropriate cell surface receptor [e.g., by tumor necrosis factor-α (TNF-α)], the IKK complex consisting of NEMO, IKKα, and IKKβ becomes activated. This IKK complex then phosphorylates IκBα, leading to its ubiquitination and flagging it for degradation by the 26S proteasome. On degradation of IκBα, NF-κB is released and translocates to the nucleus to activate gene expression. Targets of NF-κB include many antiapoptotic and pro-proliferation genes, and this pathway is constitutively activated in many human cancers (33–35). For this reason, NF-κB and the proteins that control its activation have become interesting targets for cancer drug development (39, 40).

The purpose of the present study was to further investigate the significance of our preliminary observation that NEMO associates with an active GRO. In particular, our aims were to verify that AGRO100 was associated with NEMO in treated cancer cells, to determine the biological consequences of this association, and to investigate the possible role of nucleolin in mediating it.

[4] P.J. Bates, A.C. Girvan, J.B. Klein, and W.M. Pierce, Jr., unpublished data.

Materials and Methods

Oligodeoxynucleotides

The oligodeoxynucleotides used in the present study were AGRO100, an antiproliferative GRO whose sequence is 5′-d(GGTGGTGGTGGTTGTGGTGGTGGTGG)-3′, and CRO26, an inactive (no antiproliferative activity) control oligonucleotide whose sequence is 5′-d(CCTCCTCCTCC-TTCTCCTCCTCCTCC)-3′. In some experiments, GRO15B, an inactive GRO (1–4) with sequence 5′-d(TTGGGGGGG-GTGGGT)-3′, was used as an additional control. All oligonucleotides had a phosphodiester backbone and, unless otherwise stated, were purchased in the desalted form from Integrated DNA Technologies, Inc. (Coralville, IA) and used without further purification. Oligonucleotides were resuspended in water, sterilized by filtration through a 0.2-μm filter, and then diluted with sterile water to give stock solutions (400–500 μmol/L) that were stored in aliquots at −20°C. For streptavidin precipitation experiments, the following biotin-linked versions of AGRO100, GRO15B, and CRO26 were used: 5′-biotin-d(TTTGGTGG-TGGTGGTTGTGGTGGTGGTGG)-3′, 5′-biotin-d(TTGG-GGGGGGTGGGT)-3′, and 5′-biotin-d(TTTCCTCCTCC-TCCTTCTCCTCCTCCTCC)-3′ (all from Integrated DNA Technologies).

Cell Culture and Treatment

Cell lines used were HeLa (human cervical cancer), DU145 (human prostate cancer), A549 (human non–small cell lung cancer), MCF-7 (human breast cancer), and Hs27 (nonmalignant human skin fibroblasts), which were obtained from the American Type Culture Collection (Manassas, VA). Cells were grown in a standard incubator in DMEM (Life Technologies, Chicago, IL) supplemented with 10% heat-inactivated (65°C for 20 minutes) fetal bovine serum (Life Technologies) or charcoal-stripped fetal bovine serum (for MCF-7 only; Biomeda, Foster City, CA), 100 units/mL penicillin, and 100 units/mL streptomycin. For the cell proliferation assays (Fig. 1), cells were plated at low density (1,000 or 2,000 cells per well for MCF-7 and Hs27, respectively) in 96-well plates and incubated 18 hours at 37°C to allow adherence. They were treated by addition of AGRO100 directly to the culture medium to give the final concentration indicated in the figure. Cells were incubated for a further 5 days in the presence of oligonucleotide, and then proliferation was determined using the 3-(4,5-dimethylthiazol-2-yl)-2,5-diphenyltetrazolium bromide assay as described previously (1). For other experiments, unless otherwise stated, cells were plated in six-well plates at ~50% confluence and incubated 18 hours to allow adherence and then treated by addition of oligonucleotide directly to the culture medium. Where indicated, TNF-α (R&D Systems, Inc., Minneapolis, MN) was added to the culture medium for a final concentration of 7.5 ng/mL.

Identification of Candidate GRO-Associated Proteins

Extracts were prepared from HeLa cells as described previously (16). Samples (250 μg) were incubated with a biotin-linked active GRO (GRO29A) or biotin-linked inactive control oligonucleotide (GRO15B), which were

Downloaded from mct.aacrjournals.org on April 10, 2020. © 2006 American Association for Cancer Research.

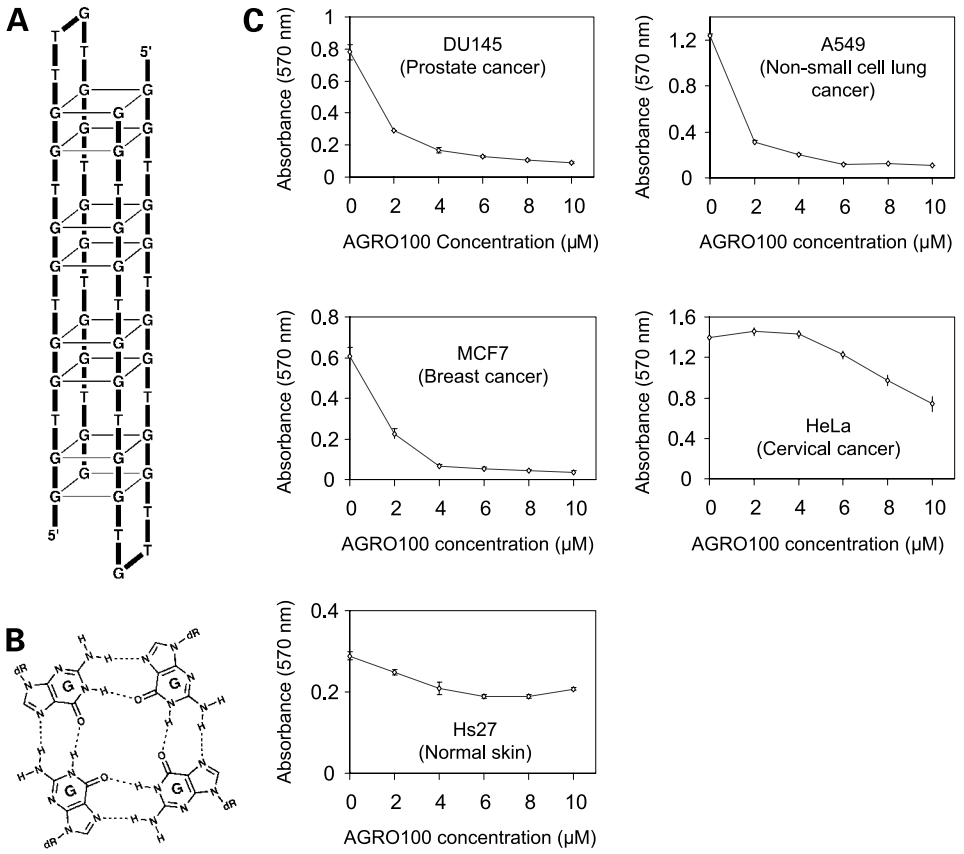

Figure 1. Structure and activity of AGRO100. **A,** structure proposed (2) for AGRO100, which comprises two strands of AGRO100 folded in antiparallel orientation to form a bimolecular quadruplex containing eight G-quartets. **B,** G-quartet showing the hydrogen bonding arrangement of the four planar guanosines. **C,** antiproliferative activity of AGRO100 in various human cell lines. Cells were incubated for 5 d following a single treatment with AGRO100 (which was added directly to the medium), and proliferation was measured using a 3-(4,5-dimethylthiazol-2-yl)-2,5-diphenyltetrazolium bromide assay. Identity of the cell line used and its origin. *Y axis,* absorbance at 570 nm, which is directly proportional to the number of viable cells in the sample. *Points,* mean of triplicate samples; *bars,* SE.

previously reported (1). The oligonucleotide-associated proteins were then captured by streptavidin precipitation (Streptavidin MagnaSphere Paramagnetic Particles, Promega, Madison, WI) and electrophoresed on SDS-polyacrylamide (8%) gels. Silver staining was used to identify bands present in the GRO29A-precipitated lane but absent in the control GRO15B lane. These bands were excised, subjected to trypsin digestion, and analyzed by matrix-assisted laser desorption ionization-time of flight mass spectrometry analysis as described previously (41). This analysis identified 18 proteins associated specifically with the active GRO, including NEMO and nucleolin. The other candidate GRO-associated proteins have not yet been verified but are currently under investigation.

Capture of Biotinylated GRO-Protein Complexes from HeLa Cells

Cells were grown to 50% confluence in T-25 flasks and treated by addition of biotinylated oligonucleotide at a final concentration of 5 μmol/L. After incubation for 2 hours at 37°C, cells were washed extensively with PBS and lysed by addition of 1 mL of lysis buffer [50 mmol/L Tris-HCl (pH 7.4), 150 mmol/L NaCl, 1 mmol/L EDTA, 1% Triton X-100, 0.5% Igepal CA630, complete protease inhibitor cocktail (Roche, Chicago, IL)]. Lysate was added to streptavidin-coated magnetic beads (MagnaBind, Pierce, Rockford, IL) and incubated 10 minutes at room temperature. Beads were captured, and unbound sample was removed. Beads were then washed thrice with 1 mL of immunoprecipitation buffer [0.1 mol/L Tris-HCl (pH 8.0), 1% (v/v) Triton X-100, 1% (w/v) deoxycholate, 0.5% (w/v) SDS, 2 mmol/L phenylmethylsulfonyl fluoride]. Finally, proteins were eluted by addition of 50 μL of loading buffer (1% SDS, 5% 2-mercaptoethanol) and boiled for 5 minutes. Captured proteins were electrophoresed on SDS-polyacrylamide (8%) gels and transferred to polyvinylidene difluoride membranes. Membranes were blocked with 5% nonfat dried milk in PBS plus 0.05% Tween 20 and then incubated with primary antibody in PBS plus 0.05% Tween 20 (1 μg/mL anti-nucleolin or 1 μg/mL anti-NEMO, both from Santa Cruz Biotechnology, Santa Cruz, CA). Following incubation with secondary antibody (0.5 μg/mL anti-mouse horseradish peroxidase conjugated, Santa Cruz Biotechnology), bands were visualized by enhanced chemiluminescence (Amersham Biosciences, Pittsburgh, PA). For densitometric quantitation, the results from three independent experiments were scanned (Epson Expression 1680, Long Beach, CA) and the intensities of bands were determined using ImageQuant 5.2 software (Amersham Biosciences). For each experiment, background (streptavidin precipitated/no oligonucleotide) was subtracted and the intensities were normalized to the value for AGRO100. Error bars shown represent the SE of the normalized results.

Downloaded from mct.aacrjournals.org on April 10, 2020. © 2006 American Association for Cancer Research.

IKK Kinase Assay

HeLa cells were plated in six-well plates as described. After 1 hour of incubation with oligonucleotide, TNF-α was added for a further 30 minutes. Cell lysates were prepared using 0.1 mol/L Tris-HCl (pH 8.0), 1% Triton X-100, 1% deoxycholate, 0.5% SDS, and 2 mmol/L phenylmethylsulfonyl fluoride. The lysates (10 μg) were then assessed for IKK kinase activity as described previously (41) using 2.5 μg of IκBα-glutathione *S*-transferase fusion protein (Santa Cruz Biotechnology) as the substrate. The gels were dried and analyzed by autoradiography or by using a phosphorimager (Typhoon 9400). For densitometric quantitation, the results from three independent experiments (as Typhoon images or scans of autoradiographic film) were analyzed using ImageQuant 5.2 software. For each experiment, intensities were normalized to the positive control (TNF-α stimulated, no oligonucleotide) and the error bars shown represent the SE of the normalized results.

Detection of Phosphorylated IκBα

HeLa cells were treated exactly as described for the IKK kinase assay. Lysates were prepared by addition of lysis buffer [62.5 mmol/L Tris-HCl (pH 6.8), 2% SDS, 10% glycerol, 50 mmol/L DTT], electrophoresed on 8% polyacrylamide-SDS gels, and transferred to polyvinylidene difluoride membrane. Standard Western blot analysis was then done using anti-phosphorylated IκBα antibody (1 μg/mL; Cell Signaling Technology, Beverly, MA) followed by analysis using anti-β-actin antibody (Sigma-Aldrich, St. Louis, MO) as a control for equal loading. For densitometric quantitation, the results from three independent experiments were scanned and the intensities of the phosphorylated IκBα and the corresponding β-actin bands were determined using ImageQuant 5.2 software. The intensity of each IκBα band was divided by the corresponding β-actin band, and for each experiment, these values were normalized to the positive control (TNF-α stimulated, no oligonucleotide). The error bars shown represent the SE of the normalized results.

Transient Transfection and Measurement of Luciferase Activity

Cells were plated in 24-well plates at a density of 2×10^4 per well and transiently transfected with a NF-κB reporter plasmid and an internal control plasmid (described below) using SuperFect reagent (Qiagen, Valencia, CA) according to the manufacturer's protocol. At 24 hours after transfection, oligonucleotide was added directly to the medium for the final concentration indicated. After 1 hour of incubation, recombinant TNF-α was added to the medium for 6 hours (where indicated) and cell lysates were prepared using reporter lysis buffer (Promega). Lysates were added to the substrate reagents supplied in the Dual-Luciferase Reporter System (Promega), and luciferase activity was measured using a luminometer (Zylux Corp., Maryville, TN). The NF-κB reporter plasmid contained tandem repeats of the κB sequence upstream of the minimal SV40 promoter and firefly luciferase gene (BD Biosciences Clontech, Palo Alto, CA). As an internal control to account for variations in transfection efficiency, pRLnull (Promega), which expresses *Renilla* luciferase by basal transcription, was used. Luciferase activities for each sample were calculated as the activity of firefly luciferase divided by *Renilla* luciferase and were normalized to the mean of the control (unstimulated) sample. The error bars shown represent SE, and Student's *t* tests[5] were used to assess the statistical significance of the reduction in activity by AGRO100 compared with the appropriate positive control (no oligonucleotide).

Electrophoretic Mobility Shift Assay for Detection of NF-κB

HeLa cells were plated in six-well plates as described. After incubation with oligonucleotide for 1 hour, TNF-α was added for a further 2 hours and then nuclear extracts were prepared as described (16). Electrophoretic mobility shift assay analysis, using radiolabeled DNA representing the NF-κB upstream response element and 10 μg nuclear extract, was done using a method that has been described previously (36). Gels were dried and analyzed by autoradiography or by using a phosphorimager (Typhoon 9400). For densitometric quantitation, the results from five independent experiments were analyzed using ImageQuant 5.2 software. For each experiment, these intensities were normalized to the control (TNF-α stimulated, no oligonucleotide) and the error bars shown represent the SE of the normalized results. For these experiments, statistical significance was calculated compared with the control oligonucleotide (CRO26) because samples were normalized to the "no oligonucleotide" samples.

Immunoprecipitation of Nucleolin

HeLa cells were plated as described. After 1 hour of incubation with oligonucleotide, TNF-α was added for a further 2 hours and then S-100 extracts were prepared (16). The extracts (100 μg) were incubated with 10 μg of anti-nucleolin antibody for 2 hours at 4°C in radioimmunoprecipitation assay buffer [150 mmol/L NaCl, 10 mmol/L Tris-HCl (pH 7.5), 0.1% SDS, 1% Triton X-100, 1% deoxycholate, 5 mmol/L EDTA, 1 mmol/L phenylmethylsulfonyl fluoride, 2 μg/mL leupeptin]. Goat anti-mouse–coated magnetic beads (MagnaBind) were then added to the samples and incubated for 1 hour at 4°C. The beads were captured, and unbound sample was removed by washing thrice with radioimmunoprecipitation assay buffer. The precipitated proteins were eluted from the beads by the addition of SDS sample loading buffer [4% SDS, 2% glycerol, 5% β-mercaptoethanol, 0.75 mol/L Tris-HCl (pH 8.8)] and heating at 65°C for 15 minutes. Western blot analysis, as described above, was then used to detect the presence of NEMO and nucleolin.

Results

Antiproliferative Activity of AGRO100

In previous work (1), we have shown that a GRO, named GRO29A, can inhibit proliferation in prostate, breast, and

[5] http://www.physics.csbsju.edu/stats/t-test.html

Downloaded from mct.aacrjournals.org on April 10, 2020. © 2006 American Association for Cancer Research.

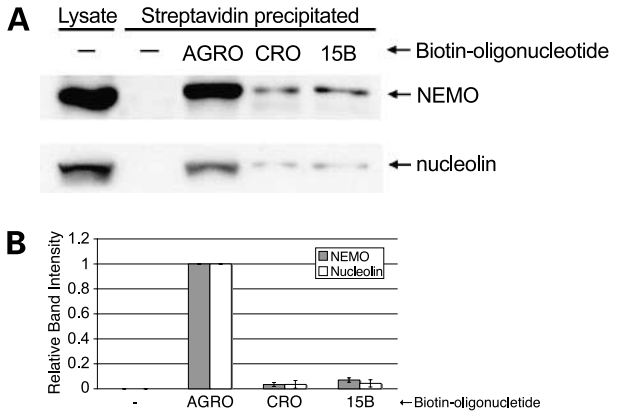

Figure 2. NEMO and nucleolin are associated with AGRO100. HeLa cells were treated with biotin-linked AGRO100 (*AGRO*) or biotin-linked control oligonucleotides [CRO26 (*CRO*) or GRO15B (*15B*)] or were untreated (–). After 2 h, cells were lysed under mild conditions and added to streptavidin-coated magnetic beads for precipitation of oligonucleotide-associated proteins. **A,** precipitated proteins were subjected to Western blot analysis to detect the presence of either NEMO or nucleolin. *Left,* nonprecipitated lysate (5 μg) was run for comparison. **B,** quantitative analysis for three independent experiments, where the intensity of bands was determined by densitometry and normalized to the AGRO band as described in Materials and Methods.

cervical cancer cells. Subsequently, we determined that the 3′-amino modification and the three 5′-thymidines of GRO29A are not necessary for nuclease resistance or biological activity (2, 4). Therefore, AGRO100, the oligonucleotide selected for clinical development, lacks these features and is an unmodified 26-mer oligodeoxynucleotide. Thermal denaturation experiments, carried out as described previously (1), indicate that AGRO100 forms a stable structure that melts at 76°C.[6] As shown schematically in Fig. 1, this structure is predicted (2) to be a bimolecular quadruplex that is stabilized by the formation of eight G-quartets. To first verify the antiproliferative activity in the cell lines of interest, AGRO100 was added directly to the culture medium and cells were incubated in the presence of the oligonucleotide for 5 days. This was followed by determination of relative cell number using a colorimetric 3-(4,5-dimethylthiazol-2-yl)-2,5-diphenyltetrazolium bromide assay. As expected, based on our previous studies of GRO29A (1–4), micromolar concentrations of AGRO100 strongly inhibited the proliferation of a variety of human cancer cells but had a lesser effect on Hs27 cells, which are nonmalignant human skin fibroblasts (Fig. 1C).

NEMO Is an AGRO100-Associated Protein

In preliminary experiments designed to identify candidate proteins that may play a role in GRO activity, we incubated biotin-linked GROs with concentrated HeLa cell extracts *in vitro*. This was followed by streptavidin precipitation, electrophoresis of captured proteins, and mass spectrometry analysis of bands that were precipitated by an active GRO but not a control oligonucleotide. Several specific GRO-associated proteins were identified by this approach, including nucleolin and NEMO (data not shown; see Materials and Methods).

To confirm that complex formation between NEMO and AGRO100 occurs in treated cancer cells, we incubated HeLa cervical carcinoma cells with biotin-linked oligonucleotides, then lysed the cells under mild conditions, and precipitated with streptavidin. Western blot analysis of the streptavidin-precipitated proteins (Fig. 2) revealed that NEMO was precipitated from cells treated with biotin-linked AGRO100 but not from untreated cells. In cells treated with biotin-linked control oligonucleotides (CRO26, an inactive C-rich oligonucleotide, or GRO15B, an inactive GRO), only a very small amount of NEMO was detected. Densitometric analyses (Fig. 2B) of three independent

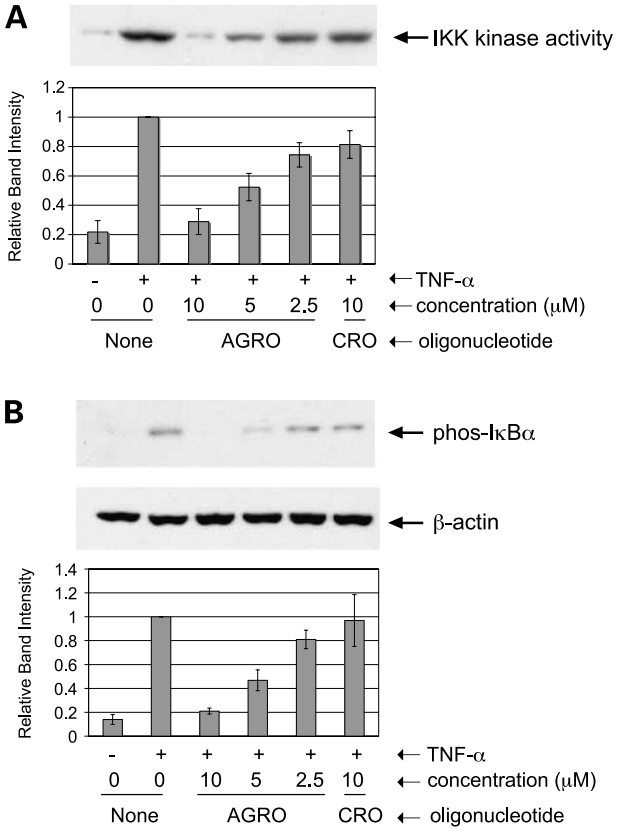

Figure 3. AGRO100 inhibits activity of the IKK complex. Lysates were prepared as described from HeLa cells that were treated for 1 h with AGRO100 (*AGRO*) or CRO26 (*CRO*) at the concentrations shown and then stimulated with TNF-α for 30 min. **A,** lysates were used in an IKK kinase assay in the presence of [γ-^{32}P]ATP and IκBα-glutathione *S*-transferase as a substrate. *Top,* IKK kinase activity as represented by phosphorylation of precipitated IκBα-glutathione *S*-transferase with ^{32}P. *Bottom,* quantified IKK kinase activity determined by densitometry of three independent experiments as described in Materials and Methods. **B,** lysates were subjected to Western blot analysis using an antibody specific for the phosphorylated form of IκBα (*phos-IκBα*) to detect IKK-mediated phosphorylation of the endogenous substrate. The blots were stripped and reanalyzed for β-actin. *Bottom,* densitometric analysis of three independent experiments as described in Materials and Methods.

[6] P.J. Bates, unpublished observation.

Downloaded from mct.aacrjournals.org on April 10, 2020. © 2006 American Association for Cancer Research.

experiments indicated that the intensity of the NEMO band precipitated by CRO26 or GRO15B was ≤7% compared with the AGRO100 sample. As expected, nucleolin was also specifically precipitated by biotin-linked AGRO100 (Fig. 2).

Inhibition of IKK Activity in AGRO100-Treated Cells

Because NEMO is essential for function of the IKK complex in the classic pathway of NF-κB signaling (38), we next investigated the effect of AGRO100 treatment on IKK activity. First, we did an IKK kinase assay, which assesses the capability of cell lysates to phosphorylate the IKK substrate IκBα in the presence of radiolabeled ATP. HeLa cells were treated for 1 hour with AGRO100 or CRO26 and then stimulated with TNF-α for 30 minutes. As seen in Fig. 3A, there was significant induction of IKK activity on stimulation with TNF-α in the absence of oligonucleotide. Incubation of cells with AGRO100 abrogated the activation of the IKK complex in a reproducible, dose-dependent manner, whereas treatment with the control CRO26 had little effect. To validate these findings, we next used an additional method to examine the IKK-mediated

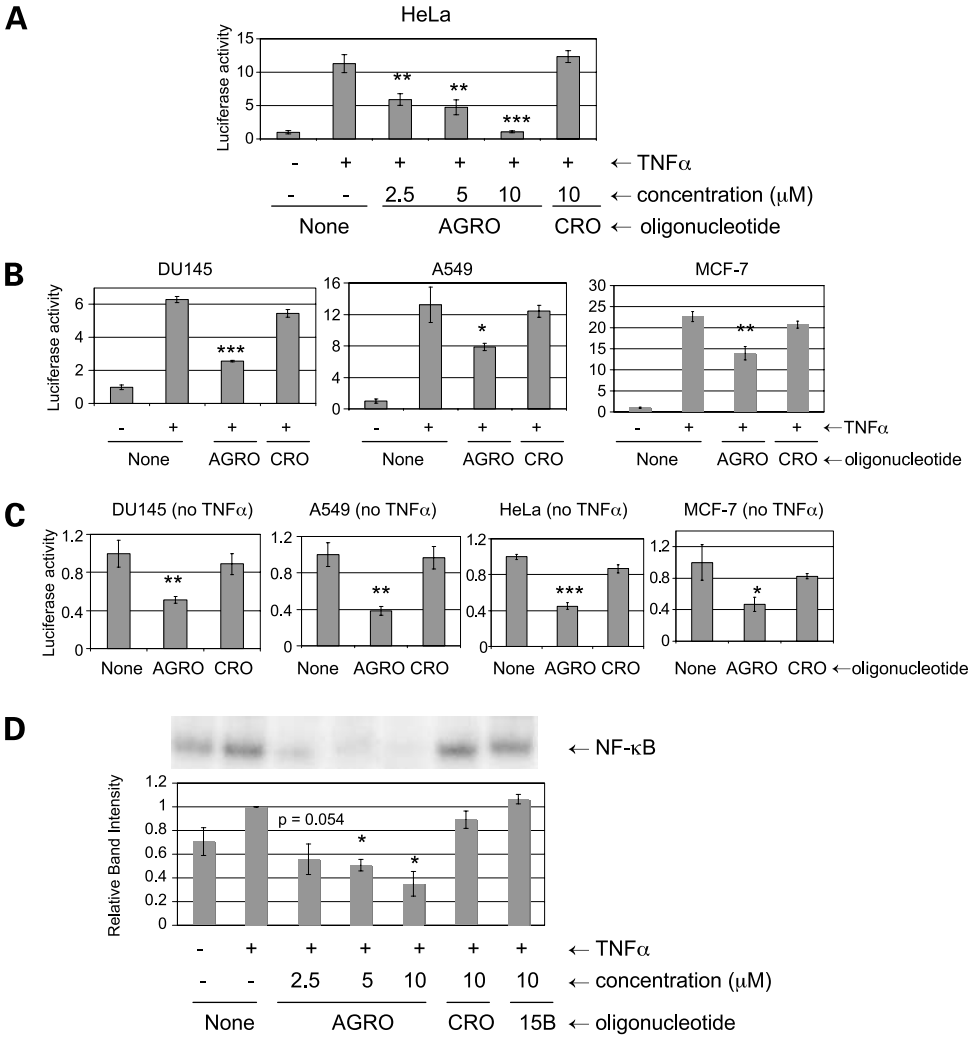

Figure 4. AGRO100 inhibits NF-κB transcriptional activity. **A,** HeLa cells were transiently transfected with a NF-κB reporter construct expressing firefly luciferase and a control plasmid expressing *Renilla* luciferase. After 24 h, cells were treated for 1 h with AGRO100 (*AGRO*) or control oligonucleotide, CRO26 (*CRO*), at the concentrations indicated and stimulated for an additional 6 h with TNF-α and luciferase activity was then measured. Luciferase activity was calculated as firefly luciferase activity divided by *Renilla* luciferase activity and shown relative to the unstimulated activity. *Columns,* mean of triplicate experiments; *bars,* SE. Statistical significance for each AGRO100-treated sample compared with control (TNF-α stimulated, no oligonucleotide). *, $P < 0.05$; **, $P < 0.01$; ***, $P < 0.001$. **B,** similar experiments were carried out in the cell lines (*top*) using 10 μmol/L AGRO100 or CRO26. Statistical significance for each AGRO100-treated sample compared with control (TNF-α stimulated, no oligonucleotide). **C,** same assays were carried out in the absence of TNF-α simulation to determine the effect of AGRO100 on constitutive NF-κB activity. Statistical significance for each AGRO100-treated sample compared with control (no oligonucleotide). **D,** nuclear extracts were prepared from HeLa cells that were treated for 1 h with AGRO100 (*AGRO*) or control oligonucleotides, CRO26 (*CRO*) or GRO15B (*15B*), and then stimulated for 2 h with TNF-α. These extracts were analyzed by electrophoretic mobility shift assay using a radiolabeled DNA duplex representing the NF-κB upstream response element to detect the presence of nuclear NF-κB. *Bottom,* densitometric analysis of five independent experiments as described in Materials and Methods and statistical significance for each AGRO100-treated sample compared with control oligonucleotide (*CRO*).

Downloaded from mct.aacrjournals.org on April 10, 2020. © 2006 American Association for Cancer Research.

phosphorylation of IκBα. Western blot analysis using an antibody specific for the phosphorylated form of IκBα was done using lysates from cells that had been treated for 1 hour with AGRO100 or CRO26 and then stimulated with TNF-α. The membrane was subsequently stripped and analyzed for β-actin to ensure that equal amounts of protein were loaded and transferred. The results (Fig. 3B) indicated that phoshorylation of IκBα occurred on stimulation with TNF-α but was reproducibly blocked by AGRO100, whereas CRO26 had no effect. These observations correlated well with the results from the IKK kinase assay.

Inhibition of NF-κB Activation in AGRO100-Treated Cells

Based on the previous result that IKK activity is inhibited, NF-κB signaling would be expected to be blocked in cancer cells treated with AGRO100. To confirm this prediction, we examined the activity of NF-κB in cells that were transiently transfected with a NF-κB-driven luciferase reporter construct. Cells were first transfected for 24 hours with the reporter construct (expressing firefly luciferase) plus an internal control vector (expressing *Renilla* luciferase) and then were treated with AGRO100 or CRO26 for 30 minutes. TNF-α was then added to the medium, and cells were incubated for a further 6 hours followed by measurement of luciferase activity. As shown in Fig. 4A, treatment of HeLa cells with AGRO100 significantly reduced TNF-α-induced NF-κB transcriptional activity in a dose-dependent manner, but treatment with the CRO26 control had no effect on NF-κB-driven luciferase activity. Next, we used the reporter gene assay to determine the effects of AGRO100 treatment on other types of cancer cells. Figure 4B shows that AGRO100 was able to significantly inhibit TNF-α-induced NF-κB activation in cell lines derived from human prostate cancer (DU145), breast cancer (MCF-7), and non–small cell lung cancer (A549). The effect on Hs27 cells was not determined because transfection efficiency in these cells was poor. Furthermore, as shown by similar experiments carried out in the absence of TNF-α, AGRO100 could also significantly inhibit constitutive NF-κB signaling in those cell lines that had significant basal NF-κB activity (Fig. 4C). In either the presence or the absence of TNF-α, there was no effect of AGRO100 on the activity due to the control *Renilla* luciferase plasmid or on cell number, therefore excluding the possibility of nonspecific effects of AGRO100 on transcription, translation, or cell viability (data not shown). Although the inhibitory effects of AGRO100 were highly reproducible (observed in at least three independent experiments for each cell line), we also used a supplementary method that did not depend on cell transfection to confirm our results. An electrophoretic mobility shift assay, using a radiolabeled DNA duplex representing the NF-κB upstream response element and nuclear extracts from HeLa cells stimulated with TNF-α, revealed induction of a band consistent with NF-κB after 2 hours of stimulation. In cells pretreated with the control oligonucleotides (CRO26 or GRO15B), nuclear NF-κB was apparent at levels similar to the cells treated with TNF-α alone. However, when the cells were treated with AGRO100 and then stimulated with TNF-α, the intensity of the NF-κB band was reduced in a dose-dependent manner (Fig. 4D).

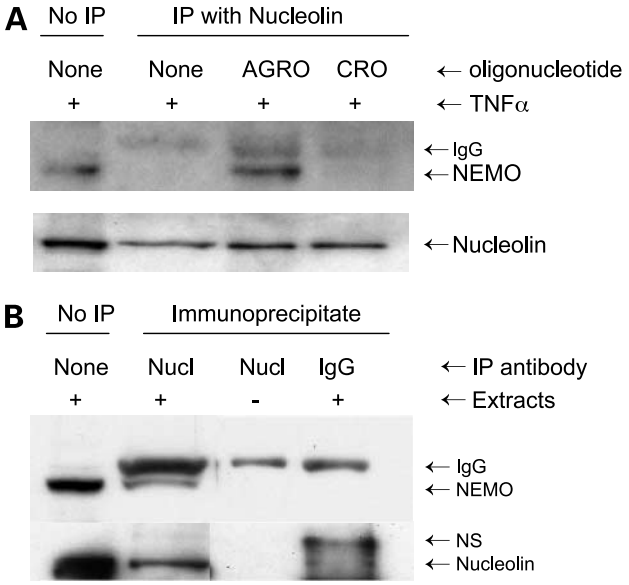

Figure 5. Coprecipitation of NEMO by nucleolin in AGRO100-treated cells. **A,** cytoplasmic (S-100) extracts were prepared from HeLa cells that had been treated for 1 h with 10 μmol/L AGRO100 (*AGRO*) or CRO26 (*CRO*) and then stimulated with TNF-α for 30 min. Immunoprecipitation (*IP*) with nucleolin antibody was done, and Western blot analysis was used to assess the presence of NEMO (48 kDa) and nucleolin (which migrates at 110 kDa). *Left,* nonprecipitated extract (5 μg) was run for comparison. **B,** to confirm the specific interaction of NEMO and nucleolin in the absence of AGRO100, a similar experiment was done. *Arrows,* lysates from HeLa cells that were stimulated 30 min with TNF-α were subjected to immunoprecipitation with nucleolin (*Nucl*) antibody, and Western blot analysis revealed the presence of NEMO and nucleolin. Mock immunoprecipitation (no cellular extracts; *lane 3*) and immunoprecipitation with nonspecific IgG (*lane 4*) were done in parallel to ensure the specificity of the interaction. *Left,* nonprecipitated lysate (5 μg) was run for comparison. *IgG* and *NS,* unrelated bands that were artifacts of the immunoprecipitation. *IgG,* mouse immunoglobulin heavy chain, ~55 kDa. *NS,* uncharacterized, nonspecific protein.

Coprecipitation of NEMO and Nucleolin from AGRO100-Treated Cells

Because both nucleolin and NEMO were precipitated by AGRO100, we proceeded to investigate the possibility that these proteins were simultaneously present in the same AGRO100-containing complex within the cell. Immunoprecipitation with nucleolin antibody was done using extracts from cells that had been treated with AGRO100 or CRO26 and then stimulated with TNF-α. The immunoprecipitates were then subjected to Western blot analysis to determine if NEMO was coprecipitated with nucleolin. Figure 5A shows that, in untreated cells or in cells treated with the control oligonucleotide, a very small amount of NEMO was detected in the nucleolin immunoprecipitate. However, when the cells were treated with AGRO100 and then stimulated with TNF-α, substantially more NEMO

Downloaded from mct.aacrjournals.org on April 10, 2020. © 2006 American Association for Cancer Research.

coprecipitated with nucleolin, indicating that NEMO, nucleolin, and AGRO100 are present in the same complex. Although we cannot definitively exclude that AGRO100 is bound independently to both proteins, a more likely explanation for this result is that AGRO100 binds directly to nucleolin and stabilizes a protein-protein interaction between nucleolin and NEMO. This idea is supported by the weak interaction between nucleolin and NEMO in untreated cells, the specificity of which was confirmed in additional experiments (Fig. 5B).

Discussion

It has become clear in recent years that NF-κB signaling is frequently deregulated in many types of cancer (33–35). NF-κB target genes encode a variety of pro-proliferation and antiapoptotic proteins, and it seems likely that malignant cells have acquired constitutive activation of this pathway to bypass the normal physiologic signals that prevent uncontrolled proliferation or to resist apoptosis induced by radiation, chemotherapy, or hormonal agents (33–35). Constitutive NF-κB activation may have particular significance with respect to advanced cancers and their resistance to therapeutic manipulation. For example, constitutive activity of NF-κB was not detected in hormone-responsive prostate cancer cell lines but was detected in hormone-insensitive prostate cancer lines and in tumor tissue from patients with advanced prostate cancer, a disease that is very often resistant to therapeutic intervention (42–44). Inhibition of NF-κB activation has also been linked to the chemopreventive properties of several compounds with activity in cancer, such as selenium, green tea, and silymarin (45–47). Down-regulation of NF-κB activity is therefore considered a very attractive strategy for developing new cancer treatments (34). The components of the IKK complex are of particular interest for drug discovery (39), and peptide inhibitors of NEMO have recently been shown to have anticancer activity (48), in addition to anti-inflammatory properties (49).

We have now shown that AGRO100 is an inhibitor of both constitutive and TNF-α-induced NF-κB signaling in a variety of cancer cell lines derived from prevalent solid tumor types. Moreover, we have defined a possible mechanism of this activity by showing that AGRO100 sequesters NEMO in a complex with nucleolin, thereby preventing activation of IKK and precluding phosphorylation of IκBα and subsequent release of NF-κB (Fig. 6B). Although it has not been ascertained that the inhibition of NF-κB is responsible for the anticancer activity of AGRO100, it seems likely that blocking this prosurvival, antiapoptotic pathway in cancer cells that have constitutive activation would lead to antiproliferative effects. It is apparent from Figs. 1 and 4 that the ability of AGRO100 to inhibit TNF-α-induced NF-κB signaling does not correlate directly with its antiproliferative activity. However, this is unsurprising because TNF-α is absent in the experiments shown in Fig. 1 and the effects of inhibiting constitutive NF-κB activity may depend complexly on numerous factors, including the basal level of NF-κB signaling and the extent of its inhibition by AGRO100. It may be significant that AGRO100 has the least growth-inhibitory effect on Hs27 cells, which have no detectable constitutive activation of NF-κB (confirmed by an electrophoretic mobility shift assay to detect NF-κB in unstimulated nuclear extracts). In any case, as we discuss below, it seems that inhibition of NF-κB signaling is one of several potential anticancer effects induced by AGRO100.

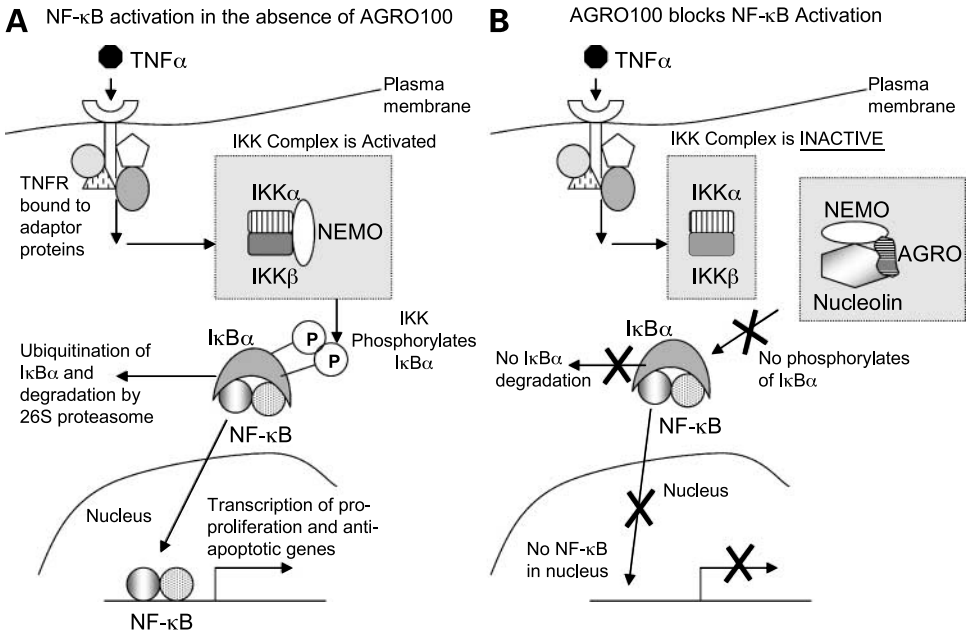

Figure 6. NF-κB activation and proposed model for its inhibition in the presence of AGRO100. **A,** on ligation of an appropriate surface receptor, such as the TNF-α receptor (*TNFR*), a signal is transduced to activate the IKK complex, which consists of IKKα, IKKβ, and NEMO. The complex then phosphorylates IκBα, which normally holds NF-κB in an inactive state in the cytoplasm, and causes it to become ultimately degraded by the 26S proteasome. Thus, the nuclear localization signal of NF-κB is unmasked and the transcription factor translocates to the nucleus to activate gene expression. **B,** in the presence of AGRO100, NEMO is sequestered in a complex containing nucleolin and AGRO100. The IKK complex is therefore inactive, and phosphorylation of IκBα cannot occur, which prevents release and activation of NF-κB.

Downloaded from mct.aacrjournals.org on April 10, 2020. © 2006 American Association for Cancer Research.

Clearly, more research is needed to fully characterize the mechanism of GROs, such as AGRO100, but the results described herein are consistent with our theory that they work primarily as nucleolin-targeted aptamers. While investigating the role of nucleolin in GRO activity, we have observed that the presence of AGRO100 can induce changes in the protein-protein interactions of nucleolin, which include some enhanced and some reduced interactions.[7] Therefore, our hypothesis about the mechanism of GROs is that their antiproliferative effects result from their binding to nucleolin and modulation of its molecular interactions. We predict that this consequently alters certain activities of this highly multifunctional protein, leading to pleiotropic biological effects. Such effects may include inactivation of NF-κB signaling, inhibition of DNA replication, and induction of cell death, all of which have been reported here or previously (4). We have now shown that AGRO100 inhibits NF-κB activation, most likely by stabilizing a complex containing nucleolin and NEMO. Thus, we have identified NEMO as one of the probable partners of nucleolin whose binding is affected (enhanced in this case) by the presence of AGRO100.

The complex interactions that regulate NF-κB signaling are an area of intense interest and much has been learned about these in recent years. However, the full details of the pathway, especially the mechanisms leading to IKK activation, are not yet fully understood. Although nucleolin has not previously been implicated in NF-κB signaling, our present findings that a nucleolin-binding aptamer inhibits NF-κB activity and that nucleolin is associated with NEMO are suggestive of a role for nucleolin in regulation of the IKK complex. In conclusion, further studies seem to be warranted to define the precise nature of the nucleolin-NEMO interaction and to determine the role of nucleolin in NF-κB signaling.

[7] P.J. Bates, Y. Teng, L.K. Casson, and W.M. Pierce, Jr., unpublished observation.

Acknowledgments

We thank Dr. John O. Trent (University of Louisville, Louisville, KY) for providing the diagrams for Fig. 1.

References

1. Bates PJ, Kahlon JB, Thomas SD, Trent JO, Miller DM. Antiproliferative activity of G-rich oligonucleotides correlates with protein binding. J Biol Chem 1999;274:26369–77.

2. Dapic V, Bates PJ, Trent JO, Rodger A, Thomas SD, Miller DM. Antiproliferative activity of G-quartet-forming oligonucleotides with backbone and sugar modifications. Biochemistry 2002;41:3676–85.

3. Dapic V, Abdomerovic V, Marrington R, et al. Biophysical and biological properties of quadruplex oligodeoxyribonucleotides. Nucleic Acids Res 2003;31:2097–107.

4. Xu X, Hamhouyia F, Thomas SD, et al. Inhibition of DNA replication and induction of S phase cell cycle arrest by G-rich oligonucleotides. J Biol Chem 2001;276:43221–30.

5. Barnhart KM, Laber DA, Bates PJ, Trent JO, Miller DM. AGRO100: the translation from lab to clinic of a tumor-targeted nucleic acid aptamer. J Clin Oncol (Meet Abstr) 2004;22:3126.

6. Laber DA, Sharma VR, Bhupalam L, Taft BS, Hendler FJ, Barnhart KM. Update on the first phase I study of AGRO100 in advanced cancer. J Clin Oncol (Meet Abstr) 2005;23:3064.

7. Derenzini M, Sirri V, Trere D, Ochs RL. The quantity of nucleolar proteins nucleolin and protein B23 is related to cell doubling time in human cancer cells. Lab Invest 1995;73:497–502.

8. Pich A, Chiusa L, Margaria E. Prognostic relevance of AgNORs in tumor pathology. Micron 2000;31:133–41.

9. Trere D, Derenzini M, Sirri V, et al. Qualitative and quantitative analysis of AgNOR proteins in chemically induced rat liver carcinogenesis. Hepatology 1996;24:1269–73.

10. Srivastava M, Pollard HB. Molecular dissection of nucleolin's role in growth and cell proliferation: new insights. FASEB J 1999;13:1911–22.

11. Tuteja R, Tuteja N. Nucleolin: a multifunctional major nucleolar phosphoprotein. Crit Rev Biochem Mol Biol 1998;33:407–36.

12. Ginisty H, Sicard H, Roger B, Bouvet P. Structure and functions of nucleolin. J Cell Sci 1999;112:761–72.

13. Borer RA, Lehner CF, Eppenberger HM, Nigg EA. Major nucleolar proteins shuttle between nucleus and cytoplasm. Cell 1989;56:379–90.

14. Dumler I, Stepanova V, Jerke U, et al. Urokinase-induced mitogenesis is mediated by casein kinase 2 and nucleolin. Curr Biol 1999;9:1468–76.

15. Hovanessian AG, Puvion-Dutilleul F, Nisole S, et al. The cell-surface-expressed nucleolin is associated with the actin cytoskeleton. Exp Cell Res 2000;261:312–28.

16. Mi Y, Thomas SD, Xu X, Casson LK, Miller DM, Bates PJ. Apoptosis in leukemia cells is accompanied by alterations in the levels and localization of nucleolin. J Biol Chem 2003;278:8572–9.

17. Zhou G, Seibenhener ML, Wooten MW. Nucleolin is a protein kinase C-ζ substrate. Connection between cell surface signaling and nucleus in PC12 cells. J Biol Chem 1997;272:31130–7.

18. Barel M, Le Romancer M, Frade R. Activation of the EBV/C3d receptor (CR2, CD21) on human B lymphocyte surface triggers tyrosine phosphorylation of the 95-kDa nucleolin and its interaction with phosphatidylinositol 3 kinase. J Immunol 2001;166:3167–73.

19. Larrucea S, Cambronero R, Gonzalez-Rubio C, et al. Internalization of factor J and cellular signalization after factor J-cell interaction. Biochem Biophys Res Commun 1999;266:51–7.

20. Daniely Y, Borowiec JA. Formation of a complex between nucleolin and replication protein A after cell stress prevents initiation of DNA replication. J Cell Biol 2000;149:799–810.

21. Wang Y, Guan J, Wang H, Wang Y, Leeper D, Iliakis G. Regulation of DNA replication after heat shock by replication protein A-nucleolin interactions. J Biol Chem 2001;276:20579–88.

22. Sengupta TK, Bandyopadhyay S, Fernandes DJ, Spicer EK. Identification of nucleolin as an AU-rich element binding protein involved in bcl-2 mRNA stabilization. J Biol Chem 2004;279:10855–63.

23. Chen CY, Gherzi R, Andersen JS, et al. Nucleolin and YB-1 are required for JNK-mediated interleukin-2 mRNA stabilization during T-cell activation. Genes Dev 2000;14:1236–48.

24. Zaidi SH, Malter JS. Nucleolin and heterogeneous nuclear ribonucleoprotein C proteins specifically interact with the 3′-untranslated region of amyloid protein precursor mRNA. J Biol Chem 1995;270:17292–8.

25. Edwards TK, Saleem A, Shaman JA, et al. Role for nucleolin/Nsr1 in the cellular localization of topoisomerase I. J Biol Chem 2000;275:36181–8.

26. Takagi M, Absalon MJ, McLure KG, Kastan MB. Regulation of p53 translation and induction after DNA damage by ribosomal protein L26 and nucleolin. Cell 2005;123:49–63.

27. Kim K, Dimitrova DD, Carta KM, Saxena A, Daras M, Borowiec JA. Novel checkpoint response to genotoxic stress mediated by nucleolin-replication protein A complex formation. Mol Cell Biol 2005;25:2463–74.

28. Khurts S, Masutomi K, Delgermaa L, et al. Nucleolin interacts with telomerase. J Biol Chem 2004;279:51508–15.

29. Ishikawa F, Matunis MJ, Dreyfuss G, Cech TR. Nuclear proteins that bind the pre-mRNA 3′ splice site sequence r(UUAG/G) and the human telomeric DNA sequence d(TTAGGG)n. Mol Cell Biol 1993;13:4301–10.

30. Dickinson LA, Kohwi-Shigematsu T. Nucleolin is a matrix attachment region DNA-binding protein that specifically recognizes a region with high base-unpairing potential. Mol Cell Biol 1995;15:456–65.

31. Dempsey LA, Sun H, Hanakahi LA, Maizels N. G4 DNA binding by LR1 and its subunits, nucleolin and hnRNP D, a role for G-G pairing in immunoglobulin switch recombination. J Biol Chem 1999;274:1066–71.

Downloaded from mct.aacrjournals.org on April 10, 2020. © 2006 American Association for Cancer Research.

32. Hanakahi LA, Sun H, Maizels N. High affinity interactions of nucleolin with G-G-paired rDNA. J Biol Chem 1999;274:15908 – 12.

33. Baldwin AS. Control of oncogenesis and cancer therapy resistance by the transcription factor NF-κB. J Clin Invest 2001;107:241 – 6.

34. Yamamoto Y, Gaynor RB. Therapeutic potential of inhibition of the NF-κB pathway in the treatment of inflammation and cancer. J Clin Invest 2001;107:135 – 42.

35. Karin M, Cao Y, Greten FR, Li ZW. NF-κB in cancer: from innocent bystander to major culprit. Nat Rev Cancer 2002;2:301 – 10.

36. Shen W, Waldschmidt M, Zhao X, Ratliff T, Krieg AM. Antitumor mechanisms of oligodeoxynucleotides with CpG and polyG motifs in murine prostate cancer cells: decrease of NF-κB and AP-1 binding activities and induction of apoptosis. Antisense Nucleic Acid Drug Dev 2002;12:155 – 64.

37. Benimetskaya L, Berton M, Kolbanovsky A, Benimetsky S, Stein CA. Formation of a G-tetrad and higher order structures correlates with biological activity of the RelA (NF-κB p65) 'antisense' oligodeoxynucleotide. Nucleic Acids Res 1997;25:2648 – 56.

38. Hayden MS, Ghosh S. Signaling to NF-κB. Genes Dev 2004;18: 2195 – 224.

39. Karin M, Yamamoto Y, Wang QM. The IKK NF-κB system: a treasure trove for drug development. Nat Rev Drug Discov 2004;3:17 – 26.

40. Nakanishi C, Toi M. Nuclear factor-κB inhibitors as sensitizers to anticancer drugs. Nat Rev Cancer 2005;5:297 – 309.

41. Powell DW, Rane MJ, Joughin BA, et al. Proteomic identification of 14-3-3ζ as a mitogen-activated protein kinase-activated protein kinase 2 substrate: role in dimer formation and ligand binding. Mol Cell Biol 2003; 23:5376 – 87.

42. Gasparian AV, Yao YJ, Kowalczyk D, et al. The role of IKK in constitutive activation of NF-κB transcription factor in prostate carcinoma cells. J Cell Sci 2002;115:141 – 51.

43. Suh J, Payvandi F, Edelstein LC, et al. Mechanisms of constitutive NF-κB activation in human prostate cancer cells. Prostate 2002;52: 183 – 200.

44. Chen CD, Sawyers CL. NF-κB activates prostate-specific antigen expression and is upregulated in androgen-independent prostate cancer. Mol Cell Biol 2002;22:2862 – 70.

45. Gasparian AV, Yao YJ, Lu J, et al. Selenium compounds inhibit IκB kinase (IKK) and nuclear factor-κB (NF-κB) in prostate cancer cells. Mol Cancer Ther 2002;1:1079 – 87.

46. Yang F, Oz HS, Barve S, de Villiers WJ, McClain CJ, Varilek GW. The green tea polyphenol (−)-epigallocatechin-3-gallate blocks nuclear factor-κB activation by inhibiting IκB kinase activity in the intestinal epithelial cell line IEC-6. Mol Pharmacol 2001;60:528 – 33.

47. Dhanalakshmi S, Singh RP, Agarwal C, Agarwal R. Silibinin inhibits constitutive and TNFα-induced activation of NF-κB and sensitizes human prostate carcinoma DU145 cells to TNFα-induced apoptosis. Oncogene 2002;21:1759 – 67.

48. Agou F, Courtois G, Chiaravalli J, et al. Inhibition of NF-κB activation by peptides targeting NF-κB essential modulator (NEMO) oligomerization. J Biol Chem 2004;279:54248 – 57.

49. May MJ, D'Acquisto F, Madge LA, Glockner J, Pober JS, Ghosh S. Selective inhibition of NF-κB activation by a peptide that blocks the interaction of NEMO with the IκB kinase complex. Science 2000;289: 1550 – 4.

Downloaded from mct.aacrjournals.org on April 10, 2020. © 2006 American Association for Cancer Research.

AACR American Association for Cancer Research

Molecular Cancer Therapeutics

AGRO100 inhibits activation of nuclear factor-κB (NF-κB) by forming a complex with NF- κB essential modulator (NEMO) and nucleolin

Allicia C. Girvan, Yun Teng, Lavona K. Casson, et al.

Mol Cancer Ther 2006;5:1790-1799.

Updated version Access the most recent version of this article at:
http://mct.aacrjournals.org/content/5/7/1790

Cited articles This article cites 49 articles, 26 of which you can access for free at:
http://mct.aacrjournals.org/content/5/7/1790.full#ref-list-1

Citing articles This article has been cited by 6 HighWire-hosted articles. Access the articles at:
http://mct.aacrjournals.org/content/5/7/1790.full#related-urls

E-mail alerts Sign up to receive free email-alerts related to this article or journal.

Reprints and Subscriptions To order reprints of this article or to subscribe to the journal, contact the AACR Publications Department at pubs@aacr.org.

Permissions To request permission to re-use all or part of this article, use this link
http://mct.aacrjournals.org/content/5/7/1790.
Click on "Request Permissions" which will take you to the Copyright Clearance Center's (CCC)
Rightslink site.

Downloaded from mct.aacrjournals.org on April 10, 2020. © 2006 American Association for Cancer Research.